Geophysical Research Letters

RESEARCH LETTER
10.1029/2021GL093391

Orbital- and Millennial-Scale Changes in Lake-Levels Facilitate Earthquake-Triggered Mass Failures in the Dead Sea Basin

Yin Lu[1,2], Jasper Moernaut[1], Nicolas Waldmann[3], Revital Bookman[3], G. Ian Alsop[4], Aurélia Hubert-Ferrari[2], Michael Strasser[1], Amotz Agnon[5], and Shmuel Marco[6]

[1]Institute of Geology, University of Innsbruck, Innsbruck, Austria, [2]Department of Geography, University of Liege, Liège, Belgium, [3]Department of Marine Geosciences, University of Haifa, Haifa, Israel, [4]Department of Geology & Geophysics, University of Aberdeen, Scotland, UK, [5]Institute of Earth Sciences, The Hebrew University of Jerusalem, Jerusalem, Israel, [6]Department of Geophysics, Tel Aviv University, Tel Aviv, Israel

Key Points:

- At the orbital- and millennial-scale, variable sedimentation rates are not a preconditioning factor for earthquake-triggered mass failures
- At the centennial-to decadal-scale, earthquake-triggered mass failures are not statistically correlated with lake-level state
- At the orbital- and millennial-scale, the mass failures are more frequent during lake-level high-stands with large-amplitude fluctuations

Supporting Information:

Supporting Information may be found in the online version of this article.

Correspondence to:

Y. Lu,
Yin.Lu@uibk.ac.at;
yinlusedimentology@yeah.net

Citation:

Lu, Y., Moernaut, J., Waldmann, N., Bookman, R., Ian Alsop, G., Hubert-Ferrari, A., et al. (2021). Orbital- and millennial-scale changes in lake-levels facilitate earthquake-triggered mass failures in the Dead Sea Basin. *Geophysical Research Letters*, *48*, e2021GL093391. https://doi.org/10.1029/2021GL093391

Received 16 MAR 2021
Accepted 24 JUN 2021

Abstract The possible link between the occurrence of submarine mass failure and climate-driven factors is highly disputed. This is due largely to the lack of comprehensive records of mass failures in the geologic record for which ages, triggers, and preconditioning factors can be reliably constrained. Such controls would allow accurate testing of cause-and-effect relationships. We present a record that comprises 490 earthquake-triggered mass failure deposits from the Dead Sea depocenter over the past 220 kyr that permits a robust statistical evaluation and correlation with potential preconditioning factors. Our data set reveals that (a) at the orbital- and millennial-scale, variable sedimentation rates are not a preconditioning factor for these mass failure deposits; (b) at the centennial-to decadal-scale, earthquake-triggered mass failures can occur at any lake-level state; (c) at the orbital- and millennial-scale, the mass failures are more frequent when lake-levels were high and punctuated by large-amplitude fluctuations.

Plain Language Summary Some researchers propose that lowering sea-level leads to mass failures, while, others suggest that raising sea-level induces mass failures. In contrast, other researchers conclude that no clear correlation exists between mass failures and sea-level change as the ages of failure events are random. This dispute is due largely to the lack of comprehensive records of mass failures in the geologic record for which ages, triggers, and preconditioning factors can be reliably constrained, thus preventing the testing of cause- and -effect relationships. We present a record of mass failures from the Dead Sea center over the last 220 kyr. The high-resolution dating, combined with well-constrained trigger and preconditioning factors, makes this a unique archive for testing the different hypotheses. Our analysis indicates that mass failures can occur during seismic shaking at any lake-level state at the centennial-to decadal-scale, but are more frequent during lake-level high-stands with large-amplitude fluctuations at orbital- and millennial-scales. Furthermore, we find that sedimentation rate is not a preconditioning factor for mass failures under seismic shaking at both the orbital- and millennial-scales.

1. Introduction

Subaqueous mass failures that propagate as slides, slumps, debris flows, and turbiditic flows are major processes that transport sediments from the continental shelf and upper slope to deep basins that can have serious socioeconomic consequences (Hampton et al., 1996; Pope et al., 2017; Sammartini et al., 2019; Talling et al., 2014). Under a changing climate, it is crucial to understand the relationship between the occurrence of mass failures and climate-driven factors such as changes in water-level and sedimentation rate (Leynaud et al., 2007; Owen et al., 2007). Despite numerous investigations on this topic, several schools of opinion exist. Some researchers demonstrate that lowering sea-level can promote mass failures (Blumberg et al., 2008; Huhn et al., 2019; McHugh et al., 2002), while others suggest the opposite (Brothers et al., 2013; Neves et al., 2016; Trincardi et al., 2003).

In contrast, some researchers have documented no clear correlation between mass failure occurrence and sea-level change as the ages of failure events appear to be random (Pope et al., 2015; Urlaub et al., 2013). They suggested that an accurately dated record of subaqueous mass failure deposits from a specific setting

with the same trigger is key to understanding the possible link (Pope et al., 2015; Smith et al., 2013; Urlaub et al., 2013). In addition to the role of water-level, previous studies have suggested that sedimentation-driven overpressure on subaqueous slopes can also decrease slope stability and facilitate mass failures (Leynaud et al., 2007; Sawyer et al., 2017; Ten Brink et al., 2016), but rapid sedimentation alone cannot facilitate mass failures (Cardona et al., 2020; Stigall & Dugan, 2010).

To address the contrasting viewpoints and interpretations noted above regarding the role of climate in driving mass failure frequency, we present a record from the Dead Sea depocenter that spans the last 220 kyr and comprises 490 earthquake-triggered (seismogenic) mass failure events. This case study provides a unique opportunity to shed new light on the debate by distinguishing and separating trigger and preconditioning factors. First, we focus on one specific setting in which the sediments experienced the same climatic and tectonic forcing (Lu, Bookman, et al., 2020; Lu, Waldmann, Ian Alsop, & Marco, 2017; Lu, Waldmann, Nadel, & Marco, 2017; Lu, Wetzler, et al., 2020). Second, it is established that earthquakes act as the trigger for these events (Lu, Waldmann, Ian Alsop, & Marco, 2017; Lu, Wetzler, et al., 2020; Lu et al., 2021). Third, the sedimentary sequence is well-dated (Goldstein et al., 2020) (Figure S1, Table S1). Fourth, the slope morphology of the basin (Sade et al., 2014) and sedimentary processes at the lake margin (Alsop et al., 2016; Haliva-Cohen et al., 2012) and center (Lu, Waldmann, Ian Alsop, & Marco, 2017; Neugebauer et al., 2014) are well-understood. Therefore, this unique record allows a critical assessment and testing of the links between the occurrence of mass failure, changes in water-level, and sedimentation rate driven by a changing climate.

2. Mass Failure Deposits in the Dead Sea

The central and deepest part of the Dead Sea marks the depocenter of the Dead Sea Basin, which is the largest pull-apart basin developed along the Dead Sea Fault (Figure 1) (Bartov et al., 2006; Ben-Avraham et al., 2008). The Dead Sea is characterized by lake-level high-stands with large-amplitude fluctuations (>140 m) during glacials, while low-stands with low-amplitude fluctuations (<70 m) occurred during interglacials (Torfstein, Goldstein, Stein, & Knzel 2013; Torfstein, 2019; Waldmann et al., 2010). Aragonite-detritus laminae mainly accumulate during glacials, while halite and homogeneous mud are more widely deposited during interglacials (Kiro et al., 2015; Torfstein et al., 2015).

Seismites in the Dead Sea comprise two categories: one group results from in situ coseismic sedimentary effects (in situ seismites: in situ folded layers, intraclast breccia layers, and micro-faults) (Ken-Tor et al., 2001; Lu, Waldmann, Ian Alsop, & Marco, 2017; Lu, Wetzler, et al., 2020; Marco & Agnon, 1995; Wetzler et al., 2010), and the other group forms by secondary seismogenic sedimentary effects, that is, seismogenic mass failure deposits (Lu, Waldmann, Ian Alsop, & Marco, 2017; Lu et al., 2021). We subdivide seismogenic mass failure deposits in the Dead Sea into four basic types.

(a) Type I: Seismogenic sandy turbidites. These deposits comprise sandy turbidites that overlie in situ seismites (Lu et al., 2021) (Figures 2a and 2b), with further sandy turbidites that correlate to historic earthquakes (Lu, Wetzler, et al., 2020) (Figures 2c and 2d). (b) Type II: Laminae fragments-imbedded detritus layers (Figures 2e–2i). These deposits are characterized by sparse fragments of aragonite-detritus laminae within detritus beds and are formed by seismogenic slope failure-induced comminution of aragonite-detritus laminae (Lu et al., 2021). (c) Type III: Slump deposits (Figure 2j). These deposits feature intensely deformed and fragmented aragonite-detritus laminae with distinctive layer folding, which are considered to be sourced from middle and lower lake slopes (Lu, Waldmann, Ian Alsop, & Marco, 2017). (d) Type IV: Chaotic deposits (Figure 2k). These deposits are characterized by mud containing coarse sands and well-rounded gravel, occasionally with some intraclasts, showing poorly sorted chaotic structures which are interpreted to be sourced from marginal lakeshore areas (Lu, Waldmann, Ian Alsop, & Marco, 2017).

In addition, thousands of intervals of homogeneous mud, turbidite, and debrite (on a centimeter to meter-scale) are also preserved in the Dead Sea depocenter (Figure S2). However, a seismic or nonseismic origin cannot yet be established for these deposits. Mixed information is expected for a combined data set that compares deposits with different triggers. To test the possible link between changes in water-level and mass failures with the same trigger (Pope et al., 2015; Urlaub et al., 2013), we focus on earthquake-triggered mass failures, whereas mass failures with unclear triggering mechanism(s) are systematically excluded from the analysis.

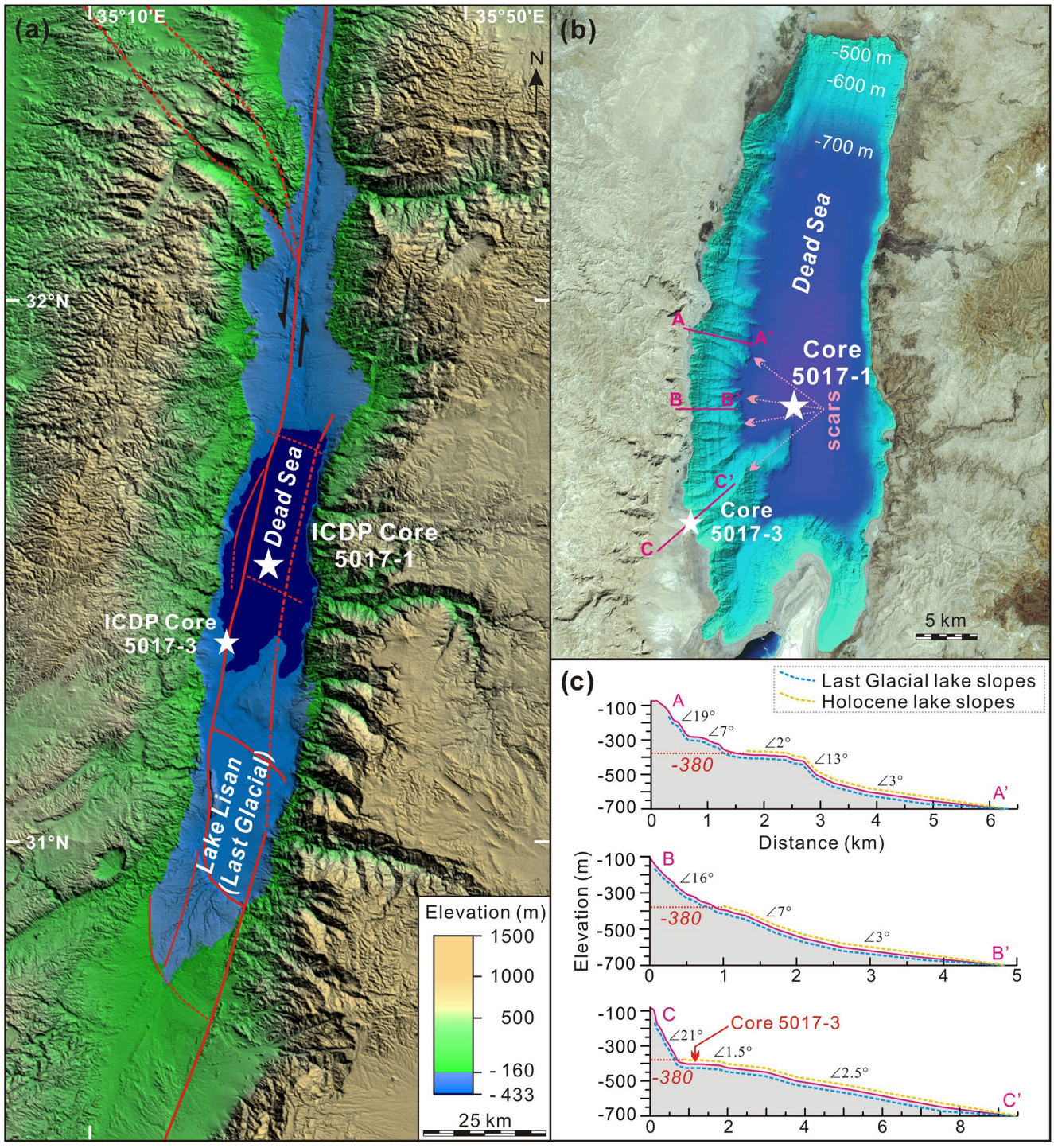

Figure 1. Tectonic setting of the Dead Sea Basin and locations of ICDP drilling. (a) Active faults (red lines) in the basin (Bartov et al., 2006; Ben-Avraham et al., 2008). (b) Bathymetric map showing the morphologic characters of basin slopes (from Sade et al., 2014) and lines of profile sections (c). (c) Profiles showing the present-day morphology of basin slopes which are used as an analog for the past 220 kyr.

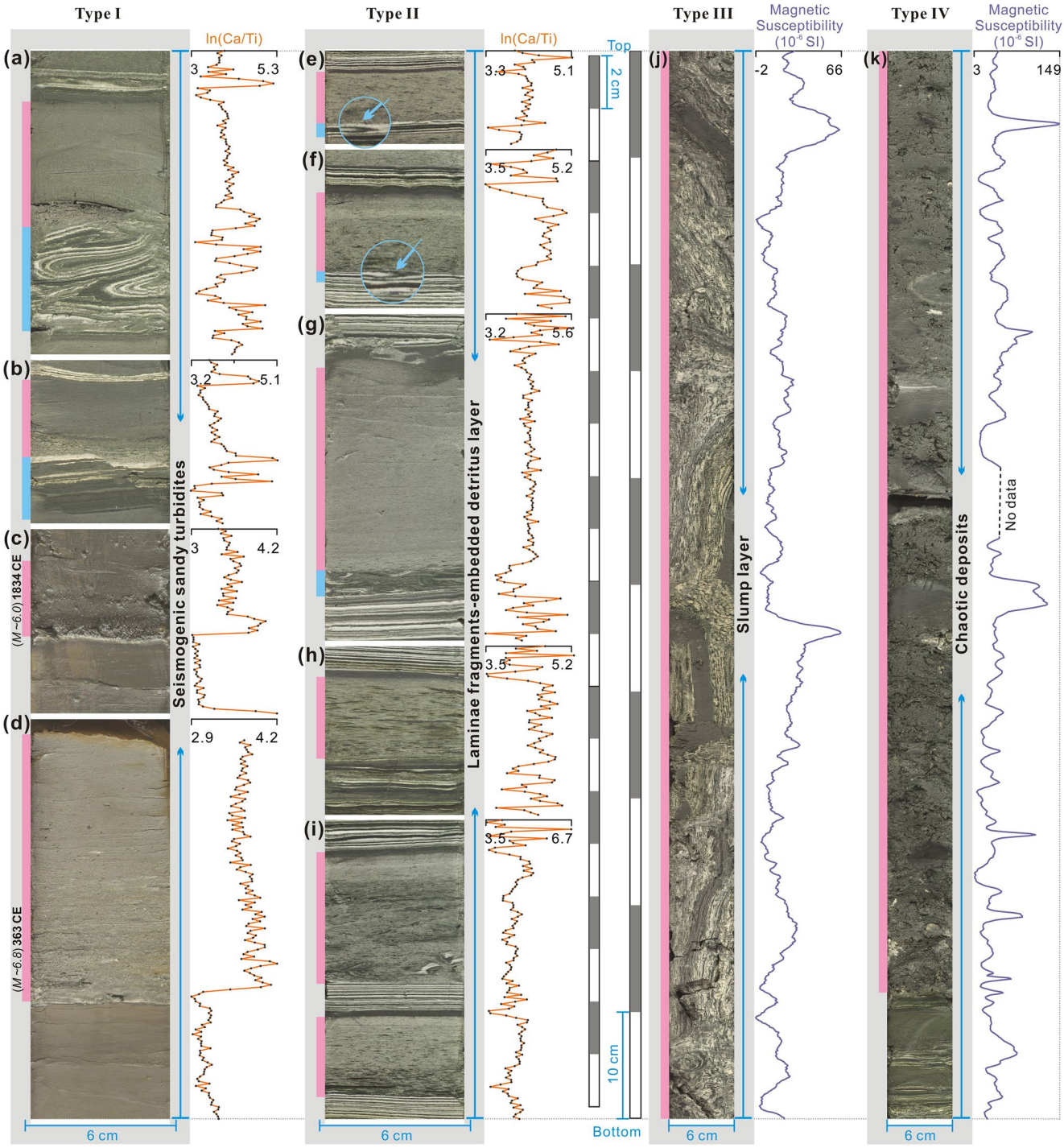

Figure 2. Features of seismogenic mass failure deposits (events) in the Dead Sea center (core 5017-1). The pink and blue bars indicate the position of events and in situ seismites, respectively. (a–d) Type I deposits. (e–i) Type II deposits; the blue circles are magnifying glasses (×2.5). (j) Type III deposits. (k) Type IV deposits. See Text S1 for core depth.

3. Materials, Methods and Chronology

3.1. ICDP Core 5017-1 (Central) and Core 5017-3 (Marginal)

During 2010–2011, a 457 m-long Core 5017-1 was recovered from the Dead Sea depocenter at a water depth of 297.5 m (Neugebauer et al., 2014). Another 340 m-long Core 5017-3 was recovered in the upper slope of

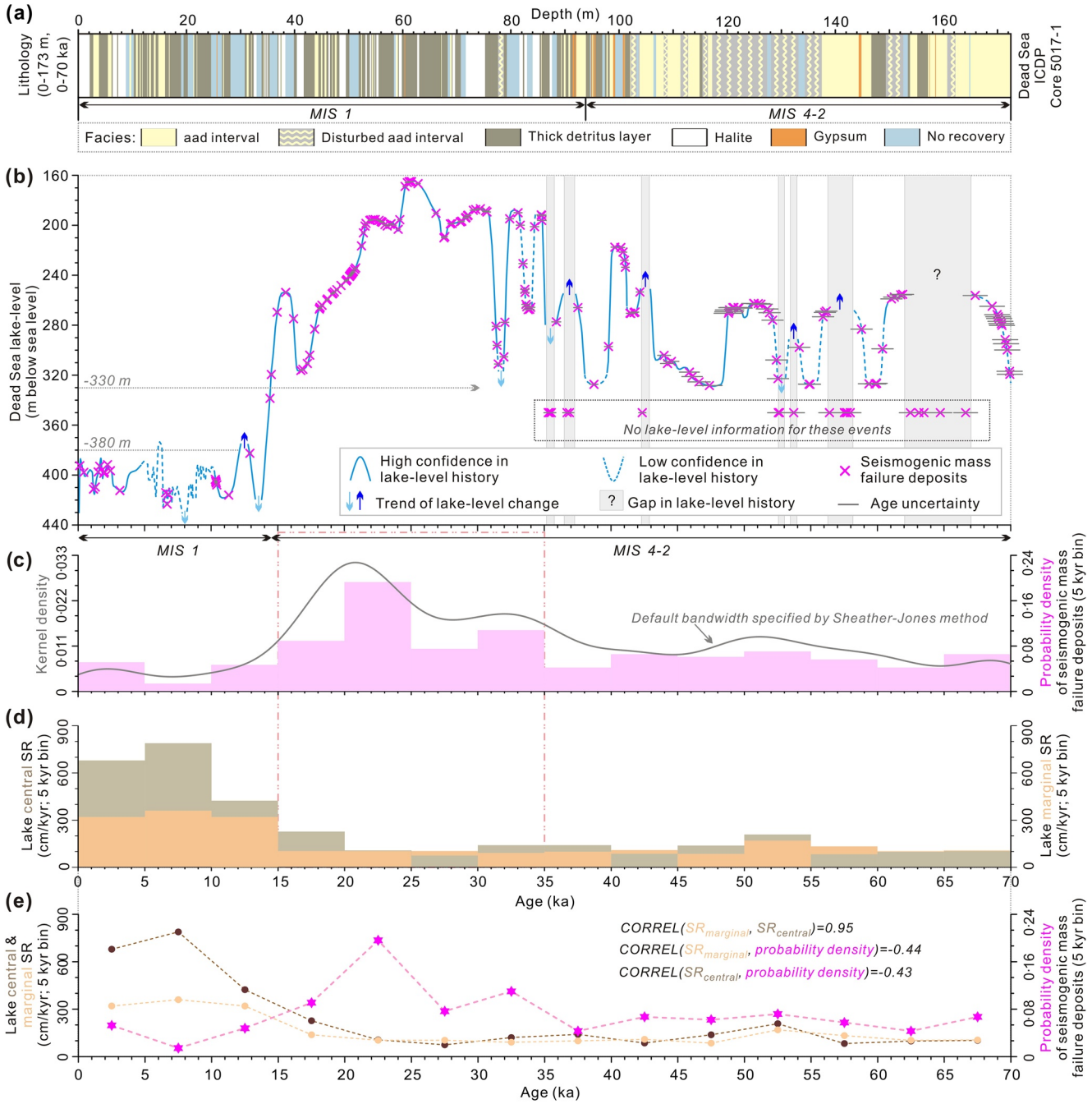

Figure 3. Distribution of seismogenic mass failure deposits (events) in the Dead Sea center over the last 70 kyr. (a) Lithology of Core 5017-1. (b) Distribution of events along with time and lake-level (Bookman et al., 2006; Torfstein, Goldstein, Kagan, & Stein, 2013; Morin et al., 2018). (c) Probability density of events in 5 kyr bins (pink-colored) and Kernel Density of events (gray curve). (d) Lake central and marginal sedimentation rate (SR). (e) Correlation between lake central SR ($SR_{central}$), lake marginal SR ($SR_{marginal}$), and probability density of events.

the lake at a water depth of 2.1 m (Figure 1). The recovered cores preserve sequences of aragonite-detritus laminae, halite, gypsum, and homogeneous mud (Figure 3a). We correlate the main stratigraphic units at the orbital-scale between the two cores based on the gamma-ray response from the downhole wireline logs (Coianiz et al., 2019). This allows us to compare sedimentation rates and facies between the two different environments in the lake.

3.2. XRF and Magnetic Susceptibility Scanning

The undisturbed core sections were scanned using an ITRAX core scanner at GFZ (Potsdam) with a Chromium tube at 30 mA current and 30 kV voltage. The scanning resolution is 1 mm and exposure time is 1 s (Neugebauer et al., 2014). We use titanium (Ti) as a proxy for clastic input and calcium (Ca) for carbonate and gypsum to investigate different facies (Lu et al., 2021). To eliminate constant-sum constraints and nonlinear matrix effects, we transform the elemental intensities into log-ratios (ln(Ca/Ti)) (Weltje et al., 2015). The core sections are also scanned at a 1-mm step for magnetic susceptibility by using a Multi-Sensor Core Logger with a Bartington MS2E sensor.

3.3. Chronology

Core 5017-1 spans the past 220 kyr (Goldstein et al., 2020; Kitagawa et al., 2017), with most dating uncertainty at $<\pm 1$ kyr (Table S1; Text S2). We constrain the timing of each mass failure event by the age of the first underlying in situ sediment horizon and by linear interpolation. In some cases, erosion occurs at the base of mass-movements and sediment gravity flows (Alsop et al., 2019; Lu, Waldmann, Ian Alsop, & Marco, 2017), thus the calculated ages constrain a maximum age for the events.

3.4. Sedimentation Rate Calculation for the Lake Center and Margin

We calculate sedimentation rate, S, as:

$$S(\Delta t) = \frac{D}{\Delta t} \tag{1}$$

where D is the cumulative thickness of sediments deposited over the time interval Δt. Sedimentation rate calculation over the past glacials and interglacials (MIS 7-1) for the lake margin is based on correlation of the main stratigraphic units between Core 5017-1 and Core 5017-3 (Coianiz et al., 2019).

Reliable millennial-scale correlations between the central and marginal cores based on gamma-ray data can only be achieved for the last 20 kyr when evaporite layers formed throughout the lake floor and can be used as stratigraphic markers. Therefore, we obtain millennial-scale variations in sedimentation rate at the lake margin over the past 70 kyr by considering both the marginal Core 5017-3 (20–0 ka) and three Last Glacial (Lisan Formation) outcrops (70–15 ka; Table S2) (Torfstein, Goldstein, Kagan, & Stein, 2013).

We average sedimentation rates derived from the three Last Glacial outcrops at a 5 kyr interval because the sections are not complete at individual sites. We then integrate the averaged outcrop record and the upper slope Core 5017-3 record into one composite record in a 5 kyr bin size (Text S3, Table S2). We use this composite record to represent sedimentation rates on the upper lake slopes for the time 70–0 ka.

3.5. Data Binning and Probability Density Calculation for Events Over the Last 70 kyr

The sediments deposited during the Last Glacial in both Core 5017-1 and lakeshore sections are sparsely dated with gaps around 5 kyr. To compare the probability density of seismogenic mass failure deposits (hereafter referred to as events) with lake center and margin sedimentation rates, we group our data set of sedimentation rates and the events in 5 kyr bins.

We calculate probability density of events, P as:

$$P(\Delta t) = \frac{n(\Delta t)}{N} \tag{2}$$

where n is the number of events over time interval Δt (=5 kyr) and N is the total number of events over the last 70 kyr. We define the probability density of events as extremely low or the highest when the values are ≤ 0.04 (standard deviation) and ≥ 0.08, respectively.

We compare the distribution of probability density of events in different sizes of bins (3.5, 5, 7 kyr). The three sets show similar distributions of probability density of events over the last 70 kyr (Figure S3), suggesting that the shape of the event distribution is insensitive to changes in bin size. In addition, we also use the Gaussian Kernel and the Sheather-Jones method to determine the optimal bandwidth (3.01) and model the Kernel Density of events. The modeling yields a smooth curve that shows a similar distribution with the probability density of events binned in different sizes (Figure S3).

4. Results

4.1. Features of Seismogenic Mass Failure Deposits (Events)

Type I deposits show smaller fluctuations in Ca/Ti ratio than the aragonite-detritus laminae intervals (Figures 2a and 2b), suggesting mixing processes. Type II deposits also show smaller fluctuations in the Ca/Ti ratio than the aragonite-detritus laminae intervals underlying the units (Figures 2e–2i), thus also suggesting mixing. Type III and IV deposits both show frequent variations in magnetic susceptibility (Figures 2j and 2k), indicating large-scale mixing processes and implying that the units have undergone significant transportation. We identify 490 such deposits in Core 5017-1 over the past 220 kyr.

4.2. Lake Margin and Center Sedimentation Rates Over the Last 220 kyr

At a millennial-scale, over the past 70 kyr, lake margin and center sedimentation rates show a similar trend, with a correlation factor of 0.95 (Figure 3e). The sedimentation rates are high during 15–0 ka (lake margin: >320 cm/kyr; center: >420 cm/kyr) and low during 70–15 ka (lake margin: <170 cm/kyr; center: <295 cm/kyr) (Figure 3d; Table S2). At an orbital-scale, over MIS 7-1, lake margin and center sedimentation rates also show a similar trend, with a correlation factor of 0.99 (Figure 4f). The rates are high during interglacials (165–645 cm/kyr) and low during glacials (<145 cm/kyr) (Figure 4e; Table S3).

4.3. Occurrence of Events Compared to Lake Levels and Sedimentation Rates During 70–0 ka

We identify 30 Type I events, 114 Type II events, 57 Type III events, and 8 Type IV events over the last 70 kyr (Figures 3b and S2; Table S4). The Type II and III events mainly occur during the Last Glacial (Figure S2). The lake-level underwent high-amplitude fluctuations (>140 m; Text S4) during the Last Glacial high-stand, compared to low-amplitude fluctuations (<70 m) during the Holocene low-stand (Figure 3b) (Torfstein, Goldstein, Kagan, & Stein, 2013). At the centennial-to decadal-scale, the events occurred at all lake-level states of rising, falling, and stable intervening periods (<5 m/kyr; Text S4).

At a millennial-scale, the events have the highest probability density (>0.08) during 35–15 ka when lake-levels show the largest fluctuations but sedimentation rates are low (Figures 3c and 3d; Table S5). In addition, the probability density is extremely low (<0.04) during 15–0 ka when lake-levels show low-amplitude fluctuations but sedimentation rates are highest. The events also occurred frequently (0.04–0.11) during 70–35 ka, when sedimentation rates are low but lake-levels display frequent middle-magnitude fluctuations. The correlation coefficients between the probability density of events and the marginal and central sedimentation rates are both −0.4, indicating a weak negative correlation between them (Figure 3e). Additionally, we find no clear relationship between the thickness of event deposits and lake-level (coefficient: −0.02), and between the thickness of event deposits and marginal sedimentation rates (coefficient: −0.25) (Figures 4a and 4b).

During 42–0 ka, dating uncertainties are <±0.3 kyr (Table S1) and there is high confidence in lake-level history for the majority (70%) of the time interval, with low confidence for the remaining 22%, and only 8% of lake-levels unknown (Figure 3b). About 81% of failure events ($N = 115$) occurred during time intervals with high confidence in lake-level history. Among them, 87% of events ($N = 100$) occurred during lake-level rises/falls (spanning 82% of the total time), while 13% of events ($N = 15$) occurred during quiet intervals (spanning 18% of the total time) (Figure 4c). Our analysis reveals that the distribution of events over the three different lake-level states is not sensitive to the different definitions for "quiet intervals" (Figure S4; Table S6).

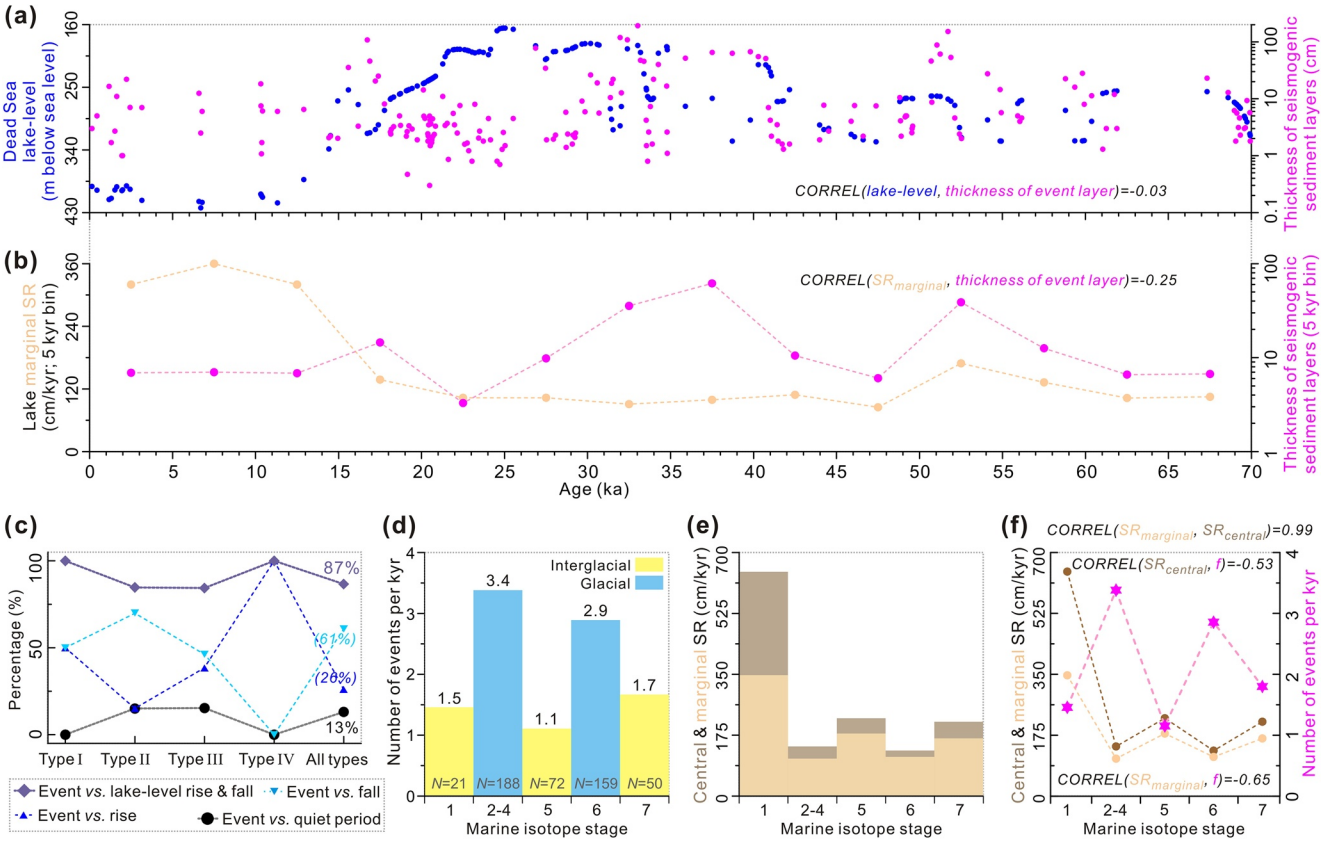

Figure 4. Occurrence of seismogenic mass failure deposits (events) in different lake-level statuses. (a and b) Correlation between the thickness of event layers, lake-level (a), and $SR_{marginal}$ (b). (c) Percentage of events occurred at different lake-level states over the past 42 kyr (high confidence in lake-level history only). (d) Frequency of events over MIS 7-1 (220–0 ka). (e) Lake marginal and central SR over MIS 7-1. (f) Correlation between $SR_{central}$, $SR_{marginal}$, and frequency of events (f) over MIS 7-1.

4.4. Occurrence of Events in the Past Glacial-Interglacial Cycles

The frequency of events in the Penultimate Interglacial (MIS 7), Penultimate Glacial (MIS 6), Last Interglacial (MIS 5), Last Glacial (MIS 4-2), and Holocene (MIS 1) are 1.5, 3.4, 1.1, 2.9, and 1.7 events per kyr, respectively (Figure 4d). The events occurred more frequently during glacials (with lake-level high-stands and large-amplitude fluctuations) than in interglacials (low-stands and low-amplitude fluctuations) (Text S5; Figure S5). The frequency of events is high during glacials when sedimentation rates are low and it is low during interglacials when sedimentation rates are high (Figures 4d–4f; Table S3). We observe negative correlations (−0.6 and −0.5) between the frequency of events and marginal and central sedimentation rates at an orbital-scale.

5. Discussion

Types I–IV events are only a partial recorder of the entire paleoearthquake catalog (Lu, Wetzler, et al., 2020), and therefore do not provide any inferences regarding earthquake recurrence. Moreover, the majority of in situ seismites in Core 5017-1 are not overlain by any types of the mass failure-related events, thereby indicating that mass failures do not develop with each significant seismic shaking or that those mass movements were too weak to reach the drill site. Therefore, some additional, nonseismic preconditioning factor(s) must have facilitated the seismically triggered mass failure deposits identified in Core 5017-1.

5.1. Implications of the Link Between Sedimentation Rates and Occurrence of Events

At the millennial-scale, the correlation coefficients between the probability density of events and lake marginal and central sedimentation rates are both −0.4 (Figure 3e). At the orbital-scale, the coefficient between the probability density of events and lake marginal sedimentation rates is −0.6, and the coefficient between the probability density of events and lake central sedimentation rates is −0.5 (Figure 4f). This new data set differs from observations in other basins where rapid sedimentation results in a reduction of submarine slope stability and thereby facilitates mass failures (Leynaud et al., 2007; Sawyer et al., 2017; Ten Brink et al., 2016). Rapid sediment loading may promote mass failures via increasing pore water pressure, thereby lowering the effective stress in a slope sequence (Leynaud et al., 2007; Sawyer et al., 2017). However, this process also depends on sediment properties (permeability and compressibility) and geometry of the slope sedimentary sequences (Flemings et al., 2002; Urlaub et al., 2015). In the Dead Sea case, comparable sedimentation rates in the basin depocenter and on the slope during MIS2-4 suggests sediment draping and thus no major changes in depositional geometry that could drive lateral fluid flow. Our data set over different time-scales suggests that variation in sedimentation rate is not the main preconditioning factor for mass failures during seismic shaking in the Dead Sea. This suggests that in combination, sedimentation rates were too low and permeability was too high for the generation of excess pore pressure and lowered effective stress in the upper lake slopes due to sedimentation alone.

5.2. Effect of Lake-Level Change on the Occurrence of Events

Our data set reveals that at the centennial- to decadal-scale, the events are not statistically correlated with lake-level state. The percentage of events that occurred during quiet intervals (13%) is close to the total time occupied by stable lake-levels (18%). Additionally, the time resolution of lake-level reconstruction and the time lag between the lake-level effects and mass failures are difficult to estimate for individual events at specific times (Text S6). Thus, the statistics at the centennial-to decadal-scale do not allow us to make a definite statement regarding a possible link between lake-level changes and mass failures. However, at the millennial- and orbital-scale, we find a statistical correlation between the lake-level and the frequency of events. Higher frequency of events (during 35–15 ka, MIS 6, and MIS 4-2) are statistically correlated with high lake-levels that were punctuated by large-amplitude falls/rises.

Field investigations and modeling in the Dead Sea Basin have confirmed that incision of stream channels and associated bank failures occurred during rapid falls in lake-level (Closson et al., 2010; Dente et al., 2021; Hassan & Klein, 2002), indicating an overall decrease in slope stability around the lake margins. A similar mechanism of falling water-levels promoting mass failures, has also been reported in Laguna Potrok Aike, southern Patagonia (Anselmetti et al., 2009), and along the continental margin of New Jersey (McHugh et al., 2002) and the South-Chilean active margin (Blumberg et al., 2008).

Previously suggested mechanisms for mass failures promoted by sea-level rise include (a) enhanced rapid sedimentation causing greater overburden on slope sediments (Nisbet & Piper, 1998; Trincardi et al., 2003), and (b) increased water load enhancing seismicity (Brothers et al., 2013; Neves et al., 2016; Smith et al., 2013). In the Dead Sea case, relatively low sedimentation rates are statistically correlated with lake-level rises and high-stands at both the millennial- and orbital-scales (Figures 3b–3d and 4e) (Lu, Bookman, et al., 2020; Lu, Waldmann, Nadel, & Marco, 2017), and thus do not support mechanism "(i)." Regarding the enhanced seismicity hypothesis, a complete paleoearthquake ($M_w \geq 5$) record that covers the Last Glacial is currently lacking and we are therefore unable to evaluate this model.

In the Dead Sea Basin, the very high lake-levels during glacials (>−330 m; Figure 3b) inundated more marginal slopes with steeper gradients (7°–21°) and loaded these slopes with loose sediments (Figures 1c and S6). These changes can increase the overall subaqueous slope failure potential during seismic shaking and lead to the accumulation of these event deposits in the lake center. Also, the rapid and high-amplitude drops in lake-level during glacials may have enhanced slope erosion and decreased terrestrial slope stability around the lake (Closson et al., 2010; Dente et al., 2021; Hassan & Klein, 2002), creating preconditioned slopes for seismogenic mass failures.

5.3. Other Lake-Level Change-Connected Factor(s) and Implications

Another important factor is that sedimentary sequences deposited under different climate conditions and lake-level states on the upper lake slopes (lake margin) comprise different lithologies. Aragonite-detritus laminae are mainly deposited during wet glacials and wet periods of interglacials when the Dead Sea lake-level is relatively high and brine is oversaturated for calcite (Barkan et al., 2001; Stein et al., 1997). The highest probability density of events occurred during 35–15 ka when lake-levels were high (> −330 m; Figure S2) and submerged more marginal slopes with steeper gradients (7°–21°) and charged these slopes with aragonite-detritus laminae.

During 35–15 ka, 66% of the events are Type II deposits which are comparable in composition to aragonite-detritus laminae (Figure 2), with thickness mostly <5 cm (Table S4), and unrelated to other typical preconditioning factor(s) for subaqueous landslides such as enhanced sedimentation rate (Figure 3). Surficial sediment remobilization triggered by earthquakes that is, reported from Chilean lakes and offshore Japan may explain these new observations of very thin layers of mixed sediments from the Dead Sea (McHugh et al., 2016; Moernaut et al., 2017; Molenaar et al., 2021). These factors connected to lake-level change can collectively favor the observed pattern of seismogenic mass failures in the Dead Sea.

Our study implies that to reliably test the cause-and-effect relationships between mass failures and climate-driven factors, for example, changes in water-level and sedimentation rate, at a much higher time-resolution, one should focus on suitable sequences. Such sequences need to comprise well-dated mass failure deposits from one setting with a well-constrained history of water-level changes at the centennial-to decadal-scale. Also needed is a quantification of preconditioning factors through (in-situ) geotechnical data and/or slope stability modeling. Our study highlights the unique potential of deep drilling and lacustrine sequences to better understand and constrain the link between mass failures and potential climate-driven factors, which can serve as an analog for marine investigations.

Data Availability Statement

Data sets are available in the Supporting Information and PANGAEA database (https://doi.org/10.1594/PANGAEA.931843).

Acknowledgments
The authors appreciate the editor L. Flesch for handling our manuscript, Ed Pope and Sebastian Cardona for constructive reviews. This research was supported by the Austrian Science Fund (FWF): M 2817 to Y. Lu and P30285-N34 to J. Moernaut, the University of Liege under Special Funds for Research, IPD-STEMA Program (R.DIVE.0899-J-F-G to Y. Lu), the Israel Science Foundation (#1645/19 to S. Marco and #1093/10 to R. Bookman), and the ICDP. A.A. is indebted to the Helmholtz Virtual Institute DESERVE for support. The authors thank C. Daxer for help modeling the Kernel Density and Nadav Wetzler for discussion.

References

Alsop, G. I., Marco, S., Weinberger, R., & Levi, T. (2016). Sedimentary and structural controls on seismogenic slumping within mass transport deposits from the Dead Sea basin. *Sedimentary Geology*, *344*, 71–90. https://doi.org/10.1016/j.sedgeo.2016.02.019

Alsop, G. I., Weinberger, R., Marco, S., & Levi, T. (2019). Identifying soft-sediment deformation in rocks. *Journal of Structural Geology*, *125*, 248–255. https://doi.org/10.1016/j.jsg.2017.09.001

Anselmetti, F. S., Ariztegui, D., De Batist, M., Catalina Gebhardt, A., Haberzettl, T., Niessen, F., et al. (2009). Environmental history of southern Patagonia unraveled by the seismic stratigraphy of Laguna Potrok Aike. *Sedimentology*, *56*(4), 873–892. https://doi.org/10.1111/j.1365-3091.2008.01002.x

Barkan, E., Luz, B., & Lazar, B. (2001). Dynamics of the carbon dioxide system in the Dead Sea. *Geochimica et Cosmochimica Acta*, *65*, 355–368. https://doi.org/10.1016/s0016-7037(00)00540-8

Bartov, Y., Agnon, A., Enzel, Y., & Stein, M. (2006). Late quaternary faulting and subsidence in the central Dead Sea basin. *Israel Journal of Earth Sciences*, *55*, 17–31. https://doi.org/10.1560/k74u-0772-1642-6282

Ben-Avraham, Z., Garfunkel, Z., & Lazar, M. (2008). Geology and evolution of the southern Dead Sea Fault with emphasis on subsurface structure. *Annual Review of Earth and Planetary Sciences*, *36*, 357–387. https://doi.org/10.1146/annurev.earth.36.031207.124201

Blumberg, S., Lamy, F., Arz, H. W., Echtler, H. P., Wiedicke, M., Haug, G. H., & Oncken, O. (2008). Turbiditic trench deposits at the South-Chilean active margin: A Pleistocene-Holocene record of climate and tectonics. *Earth and Planetary Science Letters*, *268*(3–4), 526–539. https://doi.org/10.1016/j.epsl.2008.02.007

Bookman, R., Bartov, Y., Enzel, Y., & Stein, M. (2006). Quaternary lake levels in the Dead Sea basin: Two centuries of research. *Geological Society of America Special Papers*, *401*, 155–170.

Brothers, D. S., Luttrell, K. M., & Chaytor, J. D. (2013). Sea-level-induced seismicity and submarine landslide occurrence. *Geology*, *41*(9), 979–982. https://doi.org/10.1130/G34410.1

Cardona, S., Wood, L. J., Dugan, B., Jobe, Z., Strachan, L. J., & Baas, J. (2020). Characterization of the Rapanui mass-transport deposit and the basal shear zone: Mount Messenger formation, Taranaki basin, New Zealand. *Sedimentology*, *67*(4), 2111–2148. https://doi.org/10.1111/sed.12697

Closson, D., Abou Karaki, N., & Hallot, F. (2010). Landslides along the Jordanian Dead Sea coast triggered by the lake level lowering. *Environmental Earth Sciences*, *59*(7), 1417–1430. https://doi.org/10.1007/s12665-009-0128-z

Coianiz, L., Ben-Avraham, Z., Stein, M., & Lazar, M. (2019). Spatial and temporal reconstruction of the late quaternary Dead Sea sedimentary facies from geophysical properties. *Journal of Applied Geophysics*, *160*, 15–27. https://doi.org/10.1016/j.jappgeo.2018.11.002

Dente, E., Lensky, N. G., Morin, E., & Enzel, Y. (2021). From straight to deeply incised meandering channels: Slope impact on sinuosity of confined streams. *Earth Surface Processes and Landforms*, *46*(5), 1041–1054. https://doi.org/10.1002/esp.5085

Flemings, P. B., Stump, B. B., Finkbeiner, T., & Zoback, M. (2002). Flow focusing in overpressured sandstones: Theory, observations, and applications. *American Journal of Science*, *302*(10), 827–855. https://doi.org/10.2475/ajs.302.10.827

Goldstein, S. L., Kiro, Y., Torfstein, A., Kitagawa, H., Tierney, J., & Stein, M. (2020). Revised chronology of the ICDP Dead Sea deep drill core relates drier-wetter-drier climate cycles to insolation over the past 220 kyr. *Quaternary Science Reviews*, *244*, 106460. https://doi.org/10.1016/j.quascirev.2020.106460

Haliva-Cohen, A., Stein, M., Goldstein, S. L., Sandler, A., & Starinsky, A. (2012). Sources and transport routes of fine detritus material to the late quaternary Dead Sea basin. *Quaternary Science Reviews*, *50*, 55–70. https://doi.org/10.1016/j.quascirev.2012.06.014

Hampton, M. A., Lee, H. J., & Locat, J. (1996). Submarine landslides. *Reviews of Geophysics*, *34*(1), 33–59. https://doi.org/10.1029/95rg03287

Hassan, M. A., & Klein, M. (2002). Fluvial adjustment of the Lower Jordan River to a drop in the Dead Sea level. *Geomorphology*, *45*(1–2), 21–33. https://doi.org/10.1016/s0169-555x(01)00187-8

Huhn, K., Arroyo, M., Cattaneo, A., Clare, M. A., Gràcia, E., Harbitz, C. B., et al. (2019). Modern submarine landslide complexes: A short review. In K. Ogata, A. Festa, & G. Andrea Pini (Eds.), *Submarine landslides: Subaqueous mass transport deposits from outcrops to seismic profiles* (pp. 181–200). AGU. https://doi.org/10.1002/9781119500513.ch12

Ken-Tor, R., Agnon, A., Enzel, Y., Stein, M., Marco, S., & Negendank, J. F. W. (2001). High-resolution geological record of historic earthquakes in the Dead Sea basin. *Journal of Geophysical Research*, *106*(B2), 2221–2234. https://doi.org/10.1029/2000jb900313

Kiro, Y., Goldstein, S. L., Lazar, B., & Stein, M. (2015). Environmental implications of salt facies in the Dead Sea. *The Geological Society of America Bulletin*, *128*(5–6), 824–841. https://doi.org/10.1130/b31357.1

Kitagawa, H., Stein, M., Goldstein, S. L., Nakamura, A., Lazar, B., & Party, D. S. (2017). Radiocarbon chronology of the DSDDP core at the deepest floor of the Dead Sea. *Radiocarbon*, *59*(2), 383–394. https://doi.org/10.1017/rdc.2016.120

Leynaud, D., Sultan, N., & Mienert, J. (2007). The role of sedimentation rate and permeability in the slope stability of the formerly glaciated Norwegian continental margin: The Storegga slide model. *Landslides*, *4*(4), 297–309. https://doi.org/10.1007/s10346-007-0086-z

Lu, Y., Bookman, R., Waldmann, N., & Marco, S. (2020). A 45 kyr laminae record from the Dead Sea: Implications for basin erosion and floods recurrence. *Quaternary Science Reviews*, *229*, 106143. https://doi.org/10.1016/j.quascirev.2019.106143

Lu, Y., Moernaut, J., Bookman, R., Waldmann, N., Wetzler, N., Agnon, A., et al. (2021). A new approach to constrain the seismic origin for prehistoric turbidites as applied to the Dead Sea basin. *Geophysical Research Letters*, *48*(3), e2020GL090947. https://doi.org/10.1029/2020GL090947

Lu, Y., Waldmann, N., Ian Alsop, G., & Marco, S. (2017). Interpreting soft sediment deformation and mass transport deposits as seismites in the Dead Sea depocenter. *Journal of Geophysical Research: Solid Earth*, *122*, 8305–8325. https://doi.org/10.1002/2017JB014342

Lu, Y., Waldmann, N., Nadel, D., & Marco, S. (2017). Increased sedimentation following the Neolithic Revolution in the Southern Levant. *Global and Planetary Change*, *152*, 199–208. https://doi.org/10.1016/j.gloplacha.2017.04.003

Lu, Y., Wetzler, N., Waldmann, N., Agnon, A., Biasi, G., & Marco, S. (2020). A 220,000-year-long continuous large earthquake record on a slow-slipping plate boundary. *Science Advances*, *6*(48), eaba4170. https://doi.org/10.1126/sciadv.aba4170

Marco, S., & Agnon, A. (1995). Prehistoric earthquake deformations near Masada, Dead Sea Graben. *Geology*, *23*(8), 695–698. https://doi.org/10.1130/0091-7613(1995)023<0695:pednmd>2.3.co;2

McHugh, C. M., Damuth, J. E., & Mountain, G. S. (2002). Cenozoic mass-transport facies and their correlation with relative sea-level change, New Jersey continental margin. *Marine Geology*, *184*(3), 295–334. https://doi.org/10.1016/s0025-3227(01)00240-7

McHugh, C. M., Kanamatsu, T., Seeber, L., Bopp, R., Cormier, M.-H., & Usami, K. (2016). Remobilization of surficial slope sediment triggered by the A.D. 2011 Mw9 Tohoku-Oki earthquake and tsunami along the Japan Trench. *Geology*, *44*(5), 391–394. https://doi.org/10.1130/g37650.1

Moernaut, J., Van Daele, M., Strasser, M., Clare, M. A., Heirman, K., Viel, M., et al. (2017). Lacustrine turbidites produced by surficial slope sediment remobilization: A mechanism for continuous and sensitive turbidite paleoseismic records. *Marine Geology*, *384*, 159–176. https://doi.org/10.1016/j.margeo.2015.10.009

Molenaar, A., Van Daele, M., Vandorpe, T., Degenhart, G., De Batist, M., Urrutia, R., et al. (2021). What controls the remobilization and deformation of surficial sediment by seismic shaking? Linking lacustrine slope stratigraphy to great earthquakes in South-Central Chile. *Sedimentology*. https://doi.org/10.1111/sed.12856

Morin, E., Ryb, T., Gavrieli, I., & Enzel, Y. (2018). Mean, variance, and trends of Levant precipitation over the past 4500 years from reconstructed Dead Sea levels and stochastic modeling. *Quaternary Research*, *91*(2), 751–767. https://doi.org/10.1017/qua.2018.98

Neugebauer, I., Brauer, A., Schwab, M. J., Waldmann, N. D., Enzel, Y., Kitagawa, H., et al. (2014). Lithology of the long sediment record recovered by the ICDP Dead Sea Deep Drilling Project (DSDDP). *Quaternary Science Reviews*, *102*, 149–165. https://doi.org/10.1016/j.quascirev.2014.08.013

Neves, M. C., Roque, C., Luttrell, K. M., Vázquez, J. T., & Alonso, B. (2016). Impact of sea-level rise on earthquake and landslide triggering offshore the Alentejo margin (SW Iberia). *Geo-Marine Letters*, *36*(6), 415–424. https://doi.org/10.1007/s00367-016-0459-1

Nisbet, E. G., & Piper, D. J. (1998). Giant submarine landslides. *Nature*, *392*(6674), 329–330. https://doi.org/10.1038/32765

Owen, M., Day, S., & Maslin, M. (2007). Late Pleistocene submarine mass movements: Occurrence and causes. *Quaternary Science Reviews*, *26*(7–8), 958–978. https://doi.org/10.1016/j.quascirev.2006.12.011

Pope, E. L., Talling, P. J., & Carter, L. (2017). Which earthquakes trigger damaging submarine mass movements: Insights from a global record of submarine cable breaks? *Marine Geology*, *384*, 131–146. https://doi.org/10.1016/j.margeo.2016.01.009

Pope, E. L., Talling, P. J., Urlaub, M., Hunt, J. E., Clare, M. A., & Challenor, P. (2015). Are large submarine landslides temporally random or do uncertainties in available age constraints make it impossible to tell? *Marine Geology*, *369*, 19–33. https://doi.org/10.1016/j.margeo.2015.07.002

Sade, A., Hall, J., Sade, H., Amit, G., Tibor, G., Schulze, B., et al. (2014). *Multibeam Bathymetric Map of the Dead Sea. Geological Survey of Israel report GSI/01/2014*. Retrieved from http://www.gsi.gov.il/_uploads/ftp/Maps/Shaded-batimetry_map-Dead-Sea-Poster-Front-300dpi.pdf

Sammartini, M., Moernaut, J., Anselmetti, F. S., Hilbe, M., Lindhorst, K., Praet, N., & Strasser, M. (2019). An atlas of mass-transport deposits in lakes. In K. Ogata, A. Festa, & G. Andrea Pini (Eds.), *Submarine landslides: Subaqueous mass transport deposits from outcrops to seismic profiles* (pp. 201–226). AGU. https://doi.org/10.1002/9781119500513.ch13

Sawyer, D. E., Reece, R. S., Gulick, S. P., & Lenz, B. L. (2017). Submarine landslide and tsunami hazards offshore southern Alaska: Seismic strengthening versus rapid sedimentation. *Geophysical Research Letters*, *44*(16), 8435–8442. https://doi.org/10.1002/2017gl074537

Smith, D. E., Harrison, S., & Jordan, J. T. (2013). Sea level rise and submarine mass failures on open continental margins. *Quaternary Science Reviews*, *82*(0), 93–103. https://doi.org/10.1016/j.quascirev.2013.10.012

Stein, M., Starinsky, A., Katz, A., Goldstein, S. L., Machlus, M., & Schramm, A. (1997). Strontium isotopic, chemical, and sedimentological evidence for the evolution of Lake Lisan and the Dead Sea. *Geochimica et Cosmochimica Acta*, *61*, 3975–3992. https://doi.org/10.1016/s0016-7037(97)00191-9

Stigall, J., & Dugan, B. (2010). Overpressure and earthquake initiated slope failure in the Ursa region, northern Gulf of Mexico. *Journal of Geophysical Research*, *115*(B4), B04101. https://doi.org/10.1029/2009jb006848

Talling, P., Clare, M., Urlaub, M., Pope, E., Hunt, J., & Watt, S. (2014). Large submarine landslides on continental slopes: Geohazards, methane release, and climate change. *Oceanography*, *27*(2), 32–45. https://doi.org/10.5670/oceanog.2014.38

Ten Brink, U. S., Andrews, B., & Miller, N. (2016). Seismicity and sedimentation rate effects on submarine slope stability. *Geology*, *44*(7), 563–566. https://doi.org/10.1130/g37866.1

Torfstein, A. (2019). Climate cycles in the southern Levant and their global climatic connections. *Quaternary Science Reviews*, *221*, 105881. https://doi.org/10.1016/j.quascirev.2019.105881

Torfstein, A., Goldstein, S. L., Kagan, E. J., & Stein, M. (2013). Integrated multi-site U-Th chronology of the last glacial Lake Lisan. *Geochimica et Cosmochimica Acta*, *104*, 210–231. https://doi.org/10.1016/j.gca.2012.11.003

Torfstein, A., Goldstein, S. L., Kushnir, Y., Enzel, Y., Haug, G., & Stein, M. (2015). Dead Sea drawdown and monsoonal impacts in the Levant during the last interglacial. *Earth and Planetary Science Letters*, *412*, 235–244. https://doi.org/10.1016/j.epsl.2014.12.013

Torfstein, A., Goldstein, S. L., Stein, M., & Enzel, Y. (2013). Impacts of abrupt climate changes in the Levant from Last Glacial Dead Sea levels. *Quaternary Science Reviews*, *69*, 1–7. https://doi.org/10.1016/j.quascirev.2013.02.015

Trincardi, F., Cattaneo, A., Correggiari, A., Mongardi, S., Breda, A., & Asioli, A. (2003). Submarine slides during relative sea level rise: Two examples from the eastern Tyrrhenian margin. In *Submarine mass movements and their consequences* (pp. 469–478). Springer. https://doi.org/10.1007/978-94-010-0093-2_52

Urlaub, M., Talling, P. J., & Masson, D. G. (2013). Timing and frequency of large submarine landslides: Implications for understanding triggers and future geohazard. *Quaternary Science Reviews*, *72*, 63–82. https://doi.org/10.1016/j.quascirev.2013.04.020

Urlaub, M., Talling, P. J., Zervos, A., & Masson, D. (2015). What causes large submarine landslides on low gradient (<2°) continental slopes with slow (~0.15 m/kyr) sediment accumulation? *Journal of Geophysical Research: Solid Earth*, *120*(10), 6722–6739. https://doi.org/10.1002/2015jb012347

Waldmann, N., Torfstein, A., & Stein, M. (2010). Northward intrusions of low-and mid-latitude storms across the Saharo-Arabian belt during past interglacials. *Geology*, *38*(6), 567–570. https://doi.org/10.1130/g30654.1

Weltje, G. J., Bloemsma, M., Tjallingii, R., Heslop, D., Röhl, U., & Croudace, I. W. (2015). Prediction of geochemical composition from XRF core scanner data: A new multivariate approach including automatic selection of calibration samples and quantification of uncertainties. In *Micro-XRF studies of sediment cores* (pp. 507–534). Springer. https://doi.org/10.1007/978-94-017-9849-5_21

Wetzler, N., Marco, S., & Heifetz, E. (2010). Quantitative analysis of seismogenic shear-induced turbulence in lake sediments. *Geology*, *38*(4), 303–306. https://doi.org/10.1130/g30685.1

Reference From the Supporting Information

Bookman, R., Filin, S., Avni, Y., Rosenfeld, D., & Marco, S. (2014). Possible connection between large volcanic eruptions and level rise episodes in the Dead Sea Basin. *Quaternary Science Reviews*, *89*, 123–128. https://doi.org/10.1016/j.quascirev.2014.02.009